ELSEVIER

Journal of Alloys and Compounds 275–277 (1998) 435–441

Journal of ALLOYS AND COMPOUNDS

Absorption and fluorescence of Er^{3+}-doped $LiYF_4$: measurements and simulation

M.A. Couto dos Santos[a,*], E. Antic-Fidancev[a], J.Y. Gesland[b], J.C. Krupa[c], M. Lemaître-Blaise[a], P. Porcher[a]

[a]*Laboratoire de Chimie Métallurgique et Spectroscopie des Terres Rares, CNRS UPR 209, Place Aristide Briand, 92190 Meudon, France*
[b]*Groupe de Cristallogénèse, Université du Maine, 72017 Le Mans, France*
[c]*Laboratoire de Radiochimie-IPN BP1, 91406 Orsay, France*

Abstract

Er^{3+}:$LiYF_4$ single crystal has been studied by absorption and fluorescence spectroscopy in the IR–visible-UV (0–44000 cm^{-1}) region from 4.2 K to room temperature. Polarized spectra were recorded in order to assign numerous Stark levels of electronic transitions mentioned but not attributed before in the related literature and to discuss the irreducible representations (irreps) of the $^4I_{15/2}$ sublevels. A parametric hamiltonian, including free ion (E^ν, α, β, γ, T^λ, ζ, M^k and P^i) and crystal field parameters (B_0^2, B_0^4, B_4^4, B_0^6 and B_4^6) in an approximate D_{2d} symmetry for the rare earth site in this scheelite type structure, was used to simulate 109 energy positions of the Er^{3+} ion with a r.m.s. standard deviation of 14.6 cm^{-1}. A comparison with previously published results for Nd^{3+} in the same matrix is done.

Keywords: Absorption; Fluorescence; $LiYF_4$

1. Introduction

The motivation for analyzing the $LiYF_4$ host doped with rare earth ions (RE) lies in the wide application of this matrix in laser technology [1–3]. Several works discussed the energy level scheme of the erbium trivalent ion embedded in $LiYF_4$ as well as in the stoichiometric $LiErF_4$ crystals and its simulation, but in the 0–27 000 cm^{-1} energy range [4–9]. This region constitutes only a part of the $4f^{11}$ ground configuration energy level scheme of the Er^{3+} ion which is spread up to 100 000 cm^{-1} [10,11]. This made difficult the discussion of the effective two- and three-body parameters [12], especially γ and T^3, which take into account the interaction with more excited shells [8].

The present work revisits the IR–visible-UV region of the Er^{3+} ion in the $LiYF_4$ matrix, by polarised and nonpolarised absorption and fluorescence techniques, in order to identify some crystal field states never observed in the literature. These experiments permit the assignment of the irreducible representations (irreps) of the observed Kramers' doublets, which differ from previous assignments. The attention is focused on the $^4S_{3/2}$ and $^4F_{9/2}$ levels for the experimental identification of the sublevel irreps of the ground level, $^4I_{15/2}$, and on some components of the $^4I_{9/2}$, $^4F_{7/2}$ and $^4G_{11/2}$ levels not yet detected, as well as on the $^4F_{5/2}$ level which was incorrectly assigned [4]. In the UV part of the spectrum numerous lines not assigned until now have been observed up to 44 000 cm^{-1}.

A D_{2d} point symmetry was assumed for the RE ion instead of the S_4 real one, the well known symmetry for the RE site in the scheelite type compound. This is possible because the imaginary part of the B_4^6 crystal field parameter is small [8,13]. Moreover, in order to simulate the position of the many UV energy levels it is necessary to introduce the magnetic M^k and P^i free ion parameters, which can be disregarded in the ''sister'' configuration of Nd^{3+}.

2. Experimental

The 1% Er:$LiYF_4$ and $LiErF_4$ samples have been grown by the Czochralski method, polished as a $5\times5\times5$ mm^3 cube and oriented by the Laue X-ray diffractometry. The

*Corresponding author. Post-doctoral fellowship. Present address: Instituto de Química, Universidade Estadual Paulista, PO Box 355, 14801-970 Araraquara/SP, Brazil.

0925-8388/98/$19.00
PII: S0925-8388(98)00363-6

absorption spectra in the absence of magnetic field were recorded in a Cary 2400 model spectrophotometer, with an average resolution of 0.07 nm, from IR to UV spectral region, 225–1660 nm (6500–44 000 cm^{-1}), at various temperatures, from 9 to 300 K. The polarized spectra were recorded at 4.2 K in the visible region in a Czerny–Turner type HR 1000 Jobin Yvon monochromator. The fluorescence spectra ($\lambda_{exc.}=488$ nm) were measured at liquid nitrogen temperature in a 1 m Jarrell–Ash monochromator also equipped with a R374 Hamamatsu photomultiplier, with a resolution of 0.05 nm.

3. Theoretical background

The free ion (H_{FI}) and D_{2d} crystal field (H_{CF}) hamiltonians are written in the following Eq. (1) and (2) respectively:

$$H_{FI}=H_0+\sum_{\nu=0,1,2,3}E^{\nu}(nf,nf)e_{\nu}+\alpha L(L+1)+\beta G(G_2)+\gamma G(R_7)+\sum_{\lambda=2,3,4,6,7,8}T^{\lambda}t_{\lambda}+\zeta A_{SO}+\sum_{k=0,2,4}M^{k}m_{k}+\sum_{i=2,4,6}P^{i}p_{i} \quad (1)$$

$$H_{CF}=B_0^2C_0^2+B_0^4C_0^4+B_4^4(C_4^4+C_{-4}^4)+B_0^6C_0^6+B_4^6(C_4^6+C_{-4}^6). \quad (2)$$

H_0 is the spherically symmetric part of the hamiltonian whereas E^{ν}, α, β, γ, T^{λ}, ζ, M^k and P^i are, in this sequence, the Racah, two-body and Judd's three-body free ion parameters, spin–orbit constant, Marvin integrals and spin–other orbit free ion parameters, multiplied by their angular parts. B_q^k ($k=2$, 4 and 6; $|q|\leq k$ respecting symmetry restrictions) are the real parts of the crystal field parameters and C_q^k are spherical harmonic tensors [11]. In the fitting procedure the phenomenological wave functions are obtained by diagonalisation and written on the basis of all 182 Kramers' states of the $4f^{11}$ configuration.

We have recently shown that a good r.m.s. standard deviations (σ) can be obtained for the $^2H(2)_{11/2}$ level of the Nd^{3+} ion in $LiYF_4$ [13] with neither correlated crystal field parameters nor explicit inclusion of more excited shells in the calculation [14–16], but a more complete energy level scheme has been input. The magnetic interactions have to be considered, as the $4f^{11}$ configuration has a higher number of electrons.

4. Analysis of the spectra

The symmetry properties of the rare earth ions having an odd number of electrons are described by the double groups (Kramers' states) [17]. In D_{2d} site symmetry, Γ_6 and Γ_7 are the irreps associated to the Kramers' doublets (1/2 and 3/2 in crystal quantum number μ, respectively) [18].

The observed energy levels have allowed the assignment of the ^4I_J CF states and their irreps, not completely observed until now. In Fig. 1 the absorption and fluorescence spectra of the $^4S_{3/2}$ level at 4.2, 77 and 300 K are presented. They are superimposed to make easier identification of phonons accompanying the electronic levels. If some vibronic transitions exist in the fluorescence spectrum, they have a very weak intensity and the main electronic lines attributed to the $^4I_{15/2}$ level were observed in the absorption spectrum too. Fig. 2 presents polarized and nonpolarized spectra of the $^4I_{9/2}$ level in order to point out the sublevels never observed until now and their irreps.

From Figs. 1 and 2 we can deduce that the sublevels situated at 0, 28, 320 and 355 cm^{-1} have the same irreps and the other four sublevels lying at 17, 57, 255 and 290 cm^{-1} have the same irreps, but different from the preceding ones. The positions of the two $^4S_{3/2}$ sublevels are found at 18 433 and 18 492 cm^{-1}. However, to obtain precisely the irrep of any doublet we have to consider a level with an odd number of crystal field states. The isolated $^4F_{9/2}$ level comprises five transitions corresponding to the five states present in all $^{2S+1}L_{9/2}$ levels: $3\Gamma_6+2\Gamma_7$. Its π spectrum (Fig. 3) shows three lines. Then the irreducible representation of the fundamental doublet is Γ_7, since $\Gamma_i\rightarrow\Gamma_i$ transitions are not allowed in this type of spectrum in the D_{2d} point symmetry. In the same way, by analyzing the polarized $^4S_{3/2}$ level spectra recorded between 9 and 300 K, we can conclude that the irreps of all states of the $^4I_{15/2}$ level are (increasing in energy): Γ_7, Γ_6, Γ_7, Γ_6, Γ_6, Γ_6, Γ_7 and Γ_7.

We were also able to identify the states not observed before for the $^4I_{15/2}\rightarrow{}^4I_{9/2}$ transition, by noting that the $^4I_{9/2}$ level must have only three zero-phono lines in its π-type spectrum and that the two zero-phonon lines not present must show their two satellite lines at 17 and 57 cm^{-1} in low temperature spectra. This is also true for two other electronic transitions, for example, $^4I_{15/2}\rightarrow{}^4F_{7/2}$ and $^4G_{11/2}$. Furthermore, the two lower CF states of these levels are very close to each other, suggesting a frame of fourfold degeneracy as established in the Kramers' theory. From both absorption and emission spectra 109 energy level positions were assigned (Table 1), many of them with the knowledge of their experimental irreps. In order to exploit the main component of the wave function arising from the simulation, the M_J values are also given in Table 1.

5. Simulation of the energy level scheme

The simulation of the energy level scheme was performed by considering the root mean square deviation as a factor of merit. The starting value for the free ion parameters were those of Carnall [11] whereas the cfps

Table 1
Experimental and calculated energy levels of the Er^{3+} ion in the $LiYF_4$ matrix; M_J and irreps are given too

$^{2S-1}L_J$ level	$\|M_J\|$	Γ_i	E_{exp} (cm^{-1})	E_{calc} (cm^{-1})
$^4I_{15/2}$	5/2	Γ_7	0	2
	15/2	Γ_6	17	3
	3/2	Γ_7	28	9
	1/2	Γ_6	57	48
	9/2	Γ_6	255	250
	7/2	Γ_6	290	286
	11/2	Γ_7	320	323
	13/2	Γ_7	355	342
$^4I_{13/2}$	1/2	Γ_6	6540	6553
	3/2	Γ_7	6545	6556
	13/2	Γ_7	6585	6596
	7/2	Γ_6	6680	6697
	5/2	Γ_7	6704	6718
	9/2	Γ_6	6731	6750
	11/2	Γ_7	6745	6764
$^4I_{11/2}$	1/2	Γ_6	10 213	10 217
	3/2	Γ_7	10 230	10 231
	5/2	Γ_7	10 290	10 286
	7/2	Γ_6	10 300	10 307
	11/2	Γ_7	10 309	10 313
	9/2	Γ_6	10 327	10 325
$^4I_{9/2}$	9/2	Γ_6	12 364	12 321
	3/2	Γ_7	12 486	12 475
	7/2	Γ_6	12 540	12 515
	5/2	Γ_7	12 568	12 527
	1/2	Γ_6	12 663	12 640
$^4F_{9/2}$	9/2	Γ_6	15 307	15 305
	3/2	Γ_7	15 325	15 322
	1/2	Γ_6	15 341	15 338
	7/2	Γ_6	15 416	15 415
	5/2	Γ_7	15 469	15 472
$^4S_{3/2}$	3/2	Γ_7	18 433	18 436
	1/2	Γ_6	18 492	18 493
$^2H(2)_{11/2}$	5/2	Γ_7	19 152	19 174
	7/2	Γ_6	19 172	19 198
	9/2	Γ_6	19 224	19 242
	11/2	Γ_7	19 309	19 313
	1/2	Γ_6	19 326	19 319
	3/2	Γ_7	19 342	19 332
$^4F_{7/2}$	5/2	Γ_7	20 571	20 562
	7/2	Γ_6	20 573	20 566
	3/2	Γ_7	20 662	20 659
	1/2	Γ_6	20 671	20 666
$^4F_{5/2}$	5/2	Γ_7	22 255	22 269
	3/2	Γ_7	22 279	22 287
	1/2	Γ_6	22 304	22 320
$^4F_{3/2}$	3/2	Γ_7	22 622	22 632
	1/2	Γ_6	22 653	22 663

Table 1 (continued)

$^{2S-1}L_J$ level	$\|M_J\|$	Γ_i	E_{exp} (cm^{-1})	E_{calc} (cm^{-1})
$^2G(1)_{9/2}$	9/2	Γ_6	24 531	24 512
	3/2	Γ_7	24 610	24 642
	7/2	Γ_6	24 645	24 655
	5/2	Γ_7	24 703	24 684
	1/2	Γ_6	24 756	24 773
$^4G_{11/2}$	5/2	Γ_7	26 393	26 394
	7/2	Γ_6	26 394	26 398
	9/2	Γ_6	26 458	26 458
	11/2	Γ_7	26 558	26 565
	1/2	Γ_6	26 611	26 611
	3/2	Γ_7	26 624	26 627
$^4G_{9/2}$	5/2	Γ_7	27 454	27 450
	7/2	Γ_6	27 462	27 457
+	9/2	Γ_6	27 532	27 528
	3/2	Γ_7	27 560	27 547
	1/2	Γ_6	27 571	27 565
$^2K_{15/2}$	3/2	Γ_7	–	27 579
	1/2	Γ_6	–	27 582
	15/2	Γ_6	27 844	27 844
	5/2	Γ_7	–	27 893
	7/2	Γ_6	–	27 927
	13/2	Γ_7	27 987	27 981
	11/2	Γ_7	–	28 047
	9/2	Γ_6	–	28 060
+				
$^4G_{7/2}$	1/2	Γ_6	28 132	28 133
	5/2	Γ_7	28 156	28 146
	3/2	Γ_7	28 165	28 164
	7/2	Γ_6	–	28 171
$^2P_{3/2}$	3/2	Γ_7	31 585	31 588
	1/2	Γ_6	31 651	31 656
$^2K_{13/2}$	1/2	Γ_6	32 873	32 872
	3/2	Γ_7	–	32 884
	13/2	Γ_7	33 078	33 076
+	1/2	Γ_6	–	33 112
$^2P_{1/2}$	5/2	Γ_7	33 150	33 152
	7/2	Γ_6	–	33 176
+	3/2	Γ_7	–	33 244
$^4G_{5/2}$	11/2	Γ_7	33 272	33 268
	9/2	Γ_6	–	33 296
	1/2	Γ_6	33 450	33 458
	5/2	Γ_7	–	33 508
$^4G_{7/2}$	7/2	Γ_6	–	34 047
	5/2	Γ_7	34 074	34 092
	3/2	Γ_7	34 153	34 131
	1/2	Γ_6	34 185	34 166
$^2D_{5/2}$	5/2	Γ_7	34 930	34 933
	1/2	Γ_6	34 994	34 971
	3/2	Γ_7	35 019	35 021
$^2H(2)_{9/2}$	9/2	Γ_6	36 401	36 415
	7/2	Γ_6	36 503	36 508
	5/2	Γ_7	–	36 509
	3/2	Γ_7	36 558	36 588
	1/2	Γ_6	36 684	36 672

Table 1 (continued)

$^{2S-1}L_J$ level	$\|M_J\|$	Γ_i	E_{exp} (cm^{-1})	E_{calc} (cm^{-1})
$^4D_{5/2}$	5/2	Γ_7	38 685	38 694
	1/2	Γ_6	–	38 716
	3/2	Γ_7	–	38 752
$^4D_{7/2}$	3/2	Γ_7	–	39 329
	1/2	Γ_6	39 340	39 343
	5/2	Γ_7	39 431	39 437
	7/2	Γ_6	39 552	39 545
$^2I_{11/2}$	3/2	Γ_7	41 125	41 145
	1/2	Γ_6	41 145	41 153
	7/2	Γ_6	41 205	41 218
	5/2	Γ_7	–	41 224
	9/2	Γ_6	41 285	41 269
	11/2	Γ_7	41 336	41 334
$^2L_{17/2}$	3/2	Γ_7	41 598	41 596
	1/2	Γ_6	–	41 598
	5/2	Γ_7	41 725	41 730
	7/2	Γ_6	–	41 738
	9/2	Γ_6	41 758	41 768
	11/2	Γ_7	41 830	41 810
	13/2	Γ_7	–	41 862
	15/2	Γ_6	41 902	41 914
	17/2	Γ_6	41 951	41 957
$^4D_{3/2}$	3/2	Γ_7	42 375	42 368
	1/2	Γ_6	42 410	42 403
$^2P_{3/2}$	1/2	Γ_6	–	42 953
	3/2	Γ_7	–	42 998
$^2I_{13/2}$	9/2	Γ_6	–	43 494
	3/2	Γ_7	43 526	43 507
	5/2	Γ_7	43 640	43 620
	7/2	Γ_6	43 649	43 633
	11/2	Γ_7	–	43 802
	1/2	Γ_6	43 796	43 804
	13/2	Γ_7	43 886	43 888

All values in cm^{-1}.

were taken from Ref. [13]. A first tentative without magnetic interactions showed the impossibility of reproducing the energy levels higher than 25 000 cm^{-1}, correctly. These interactions have only a minor effect on the $4f^3$ configuration of Nd^{3+}, for which the simulation of all experimental levels was made with the FI and CF parameters varying freely. However, a very good simulation is performed when M^k and P^i parameters are included, especially with a satisfying reproduction of the UV level positions. Although these magnetic parameters have considerably improved the energy level scheme fitting, not all of them vary freely. The M^k/M^0 ($k=2$, 4) and P^i/P^2 ($i=4$, 6) ratios were kept constant according to Ref. [11] ($M^2/M^0=0.56$, $M^4/M^0=0.31$, $P^4/P^2=0.50$ and $P^6/P^2=0.10$, respectively). The cf parameters vary only slightly in the rare earth series as expected in an isostructural series. All parameters are listed in Table 2.

6. Conclusion

The Er^{3+}:$LiYF_4$ crystal has been analyzed by polarized and non polarized absorption and fluorescence measurements. All crystal field states between 0–27 000 cm^{-1} were assigned, including their irreps. The irreps of the electronic levels in the UV region up to 44 000 cm^{-1} were not assigned experimentally. The phenomenological simulation was performed on 108 experimental levels with a r.m.s. value of 14.6 cm^{-1}, for 16 free ion and 5 crystal field parameters. The M^k and P^i were kept in the appropriate ratio [11]. The values of the free ion parameters are larger than in the case of the Nd^{3+} ion, as expected. This means a more important interaction between the 4f configuration and excited configurations. The calculated wave functions are not completely good because the states situated around 24 200 cm^{-1} ($^2G(1)_{9/2}$ or $^2H(2)_{9/2}$) and

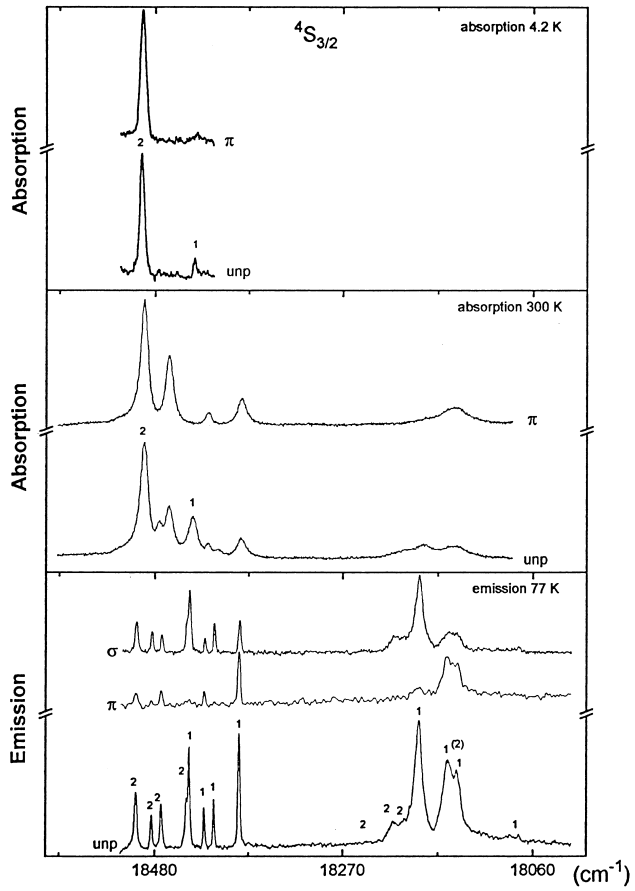

Fig. 1. Polarized and nonpolarized absorption spectra of the $^4S_{3/2}$ level at 4.2 and 300 K; emission spectra of this level at 77 K. ''1'' and ''2'' refer respectively to transitions from the $^4S_{3/2}$ sublevels to the CF components of the ground level.

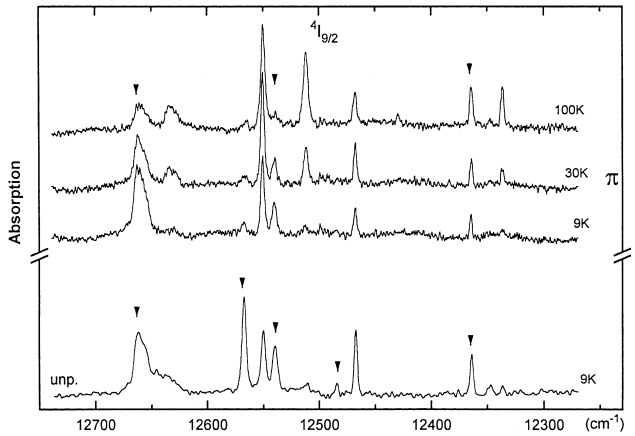

Fig. 2. Polarized and nonpolarized absorption spectra of the $^4I_{9/2}$ level at 9, 30 and 300 K.

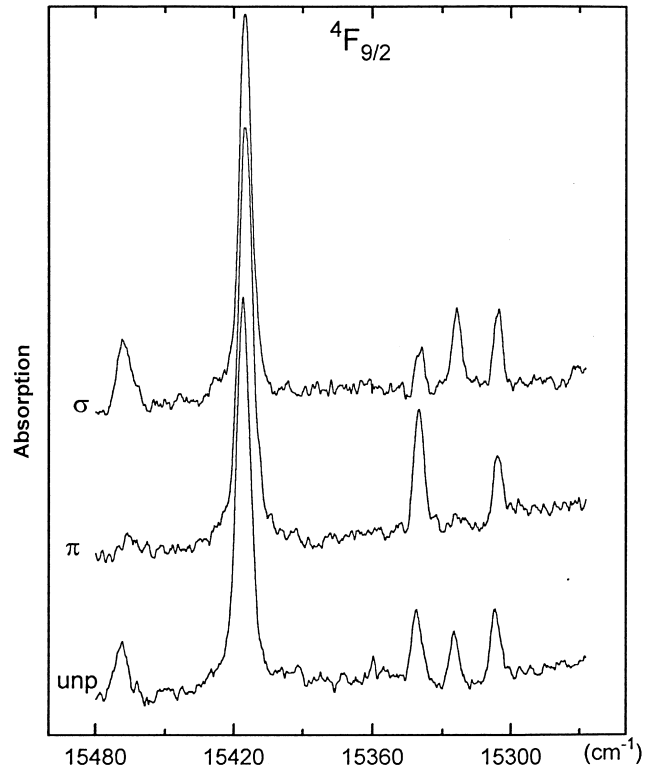

Fig. 3. Polarized and nonpolarized absorption spectra of the $^4F_{9/2}$ level at 9 K.

Table 2
Free ion and crystal field parameters of the Er^{3+} ion in an approximate D_{2d} symmetry in $LiYF_4$ matrix; the M^2/M^0, M^4/M^0, P^4/P^2 and P^6/P^2 ratios are fixed according to Ref. [11]

Parameter	Value (cm^{-1})
E^0	35 214.19
E^1	6607.22
E^2	32.99
E^3	664.86
α	18.29
β	−589.84
γ	1755.61
T^2	455.12
T^3	38.43
T^4	83.67
T^6	−348.26
T^7	243.92
T^8	388.37
ζ	2378.00
M^0	4.10
$[M^2]$	2.30
$[M^4]$	1.27
P^2	801.82
$[P^4]$	400.90
$[P^6]$	80.18
B_0^2	323.07
B_0^4	−753.83
B_4^4	−1052.24
B_0^6	−43.60
B_4^6	−623.59
Number of levels	109
r.m.s. (σ)	14.6

42 400 cm^{-1} ($^4D_{3/2}$ or $^2D(1)_{3/2}$) are always poorly defined [14]. However, for most of the energy level scheme they are probably good enough to be used in the calculation of the magnetic Zeeman splitting that we will compare to the experimental data [19].

References

[1] M.V. Petrov, A.M. Tkachuk, Opt. Spectrosc. 45 (1978) 81.
[2] F. Auzel, S. Hubert, D. Meichenen, Appl. Phys. Lett. 54 (1989) 681.
[3] F.G. Anderson, H. Weidner, P.L. Summers, R.E. Peale, J. Lumin. 62 (1994) 77.
[4] M.R. Brown, K.G. Roots, W.A. Shand, J. Phys. C: Solid State Phys. 2 (1969) 593.
[5] S.M. Kulpa, J. Phys. Chem. Solids 36 (1975) 1317.
[6] N. Karayianis, J. Phys. Chem. Solids 32 (1971) 2385.
[7] H.P. Christensen, Phys. Rev. B 19 (1979) 6564.
[8] A.A.S. da Gama, G.F. de Sá, P. Porcher, P. Caro, J. Phys. Chem. Solids 75 (1981) 2583.
[9] X. Chen, Z. Luo, J. Phys.: Condens. Matter 8 (1996) 2571.
[10] G.H. Dieke, Spectra and Energy Levels of Rare Earth Ions in Crystals, Wiley, New York, 1968.
[11] W.T. Carnall, G.L. Goodman, K. Rajnak, R.S. Rana, J. Chem. Phys. 90 (1989) 3443.
[12] B.R. Judd, Operator Techniques in Atomic Spectroscopy, McGraw-Hill, New York, 1963.
[13] M.A. Couto dos Santos, P. Porcher, J.-C. Krupa, J.-Y. Gesland, J. Phys.: Condens. Matter 8 (1996) 46.
[14] J.B. Gruber, J.R. Quagliano, M.F. Reid, F.S. Richardson, M.E. Hills, M.D. Seltzer, S.B. Stevens, C.A. Morrison, T.H. Allik, Phys. Rev. B 48 (1993) 15561.
[15] G.W. Burdick, F.S. Richardson, J. Alloys Comp. 250 (1997) 293.
[16] M. Faucher, O.K. Moune, J. Alloys Comp. 250 (1997) 306.
[17] S. Hufner, Optical Spectra of Transparent Rare Earth Compounds, Academic Press, London, 1978.
[18] P.H. Butler, Point Group Symmetry and Applications, Plenum Press, New York, 1981.
[19] M.A. Couto Dos Santos, E. Antic-Fidancev, J.Y. Gesland, J.C. Krupa, M. Lemaître-Blaise, P. Porcher (to be published).